NANO LETTERS

2008
Vol. 8, No. 2
586−590

Selective Probing and Imaging of Cells with Single Walled Carbon Nanotubes as Near-Infrared Fluorescent Molecules

Kevin Welsher,† Zhuang Liu,† Dan Daranciang, and Hongjie Dai*

Department of Chemistry, Stanford University, Stanford, California 94305

Received November 12, 2007; Revised Manuscript Received December 13, 2007

ABSTRACT

Fluorescent molecules emitting in the near-infrared (NIR, wavelength ~0.8–2 μm) are relatively scarce and have been actively sought for biological applications because cells and tissues exhibit little auto-fluorescence in this region. Here, we report the use of semiconducting single-walled carbon nanotubes (SWNTs) as near-infrared fluorescent tags for selective probing of cell surface receptors and cell imaging. Biologically inert SWNTs with polyethyleneglycol functionalization are conjugated to antibodies such as Rituxan to selectively recognize CD20 cell surface receptor on B-cells with little nonspecific binding to negative T-cells and Herceptin to recognize HER2/neu positive breast cancer cells. We image selective SWNT–antibody binding to cells by detecting the intrinsic NIR photoluminescence of nanotubes. We observe ultralow NIR autofluorescence for various cells, an advantageous feature over high autofluorescence and large variations between cells lines in the visible. This establishes SWNTs as novel NIR fluorophors for sensitive and selective biological detections and imaging in vitro and potentially in vivo. Further, our results clearly show that the interactions between carbon nanotubes and living cells are strongly dependent on surface functionalization of nanotubes.

NIR fluorescent markers promise to be of great use in biological systems due to little background signals caused by autofluorescence from cells, tissues, and other biological molecules in this spectral range, as most autofluorescence is confined to the visible.[1] Furthermore, biological tissues allow for relatively high transmission and penetration of NIR light near ~1 μm for detection within an organism or under the surface of tissues.[2] Inorganic nanostructured materials with interesting optical properties have been actively pursued in recent years for biological research.[3] It has been shown that semiconductor quantum dots such as PbSe[4] emit in the NIR range, leading to useful applications in vitro and in vivo.[5] On the other hand, semiconducting single-walled carbon nanotubes (SWNTs) are quasi one-dimensional materials with small band-gaps on the order of ~1 eV, exhibiting photoluminescence in the NIR.[6] The low toxicity[7,8] and intrinsic optical properties make SWNTs promising for multifunctional imaging and therapeutic agents.[9−11] Thus far, NIR imaging of the photoluminescence of SWNTs nonspecifically bound to live cells has been shown in vitro[12] and in rabbit tissues ex vivo.[13] It remains a wide open area to block the high nonspecific binding (NSB) nature[14−16] of as-grown or poorly passivated nanotubes, develop SWNTs into biologically inert NIR tags free of NSB, and thus retain the specificity intrinsic to biological species in association with the nanotube tags.

In this work, we report the development of antibody conjugated SWNTs as near-infrared (NIR) fluorescent labels for probing cell surface receptors with high specificity and high sensitivity. We first block nonspecific binding and obtain highly water-soluble and biologically inert SWNTs by functionalization with phospholipid−polyethyleneglycol (PEG)−amine (PL−PEG−NH_2) with long (~5400D) PEG chains. The high degree of PEGylation of SWNTs imparts high hydrophilicity and water solubility to nanotubes. We then conjugated nanotubes with Rituxan, an antibody that recognizes the CD20 cell surface receptor, and Herceptin, which recognizes the HER2/neu receptor on certain breast cancer cells. We show SWNT−antibody conjugate selectively binding to cell surface receptors by detecting the intrinsic NIR photoluminescence of SWNTs. Negligible background signals due to autofluorescence of cells in the NIR region are observed compared to SWNT photoluminescence. Little variation in the NIR autofluorescence levels is seen between different cell lines, which is in strong contrast to the high autofluorescence and large variations between cells lines in the visible. These results open up the possibility of SWNTs as novel NIR fluorophores for highly sensitive and selective biological detections and developing new imaging modalities.

As grown SWNTs are highly hydrophobic and exhibit high NSB to biological systems including proteins and cells.[14−17] It is imperative to obtain highly hydrophilic and biologically inert (i.e., NSB-free) SWNTs as NIR fluorescent tags to retain the specificity corresponding to biomolecules (e.g.,

* Corresponding author. E-mail: hdai@stanford.edu.
† These authors contributed equally to this work.

10.1021/nl072949q CCC: $40.75
Published on Web 01/16/2008

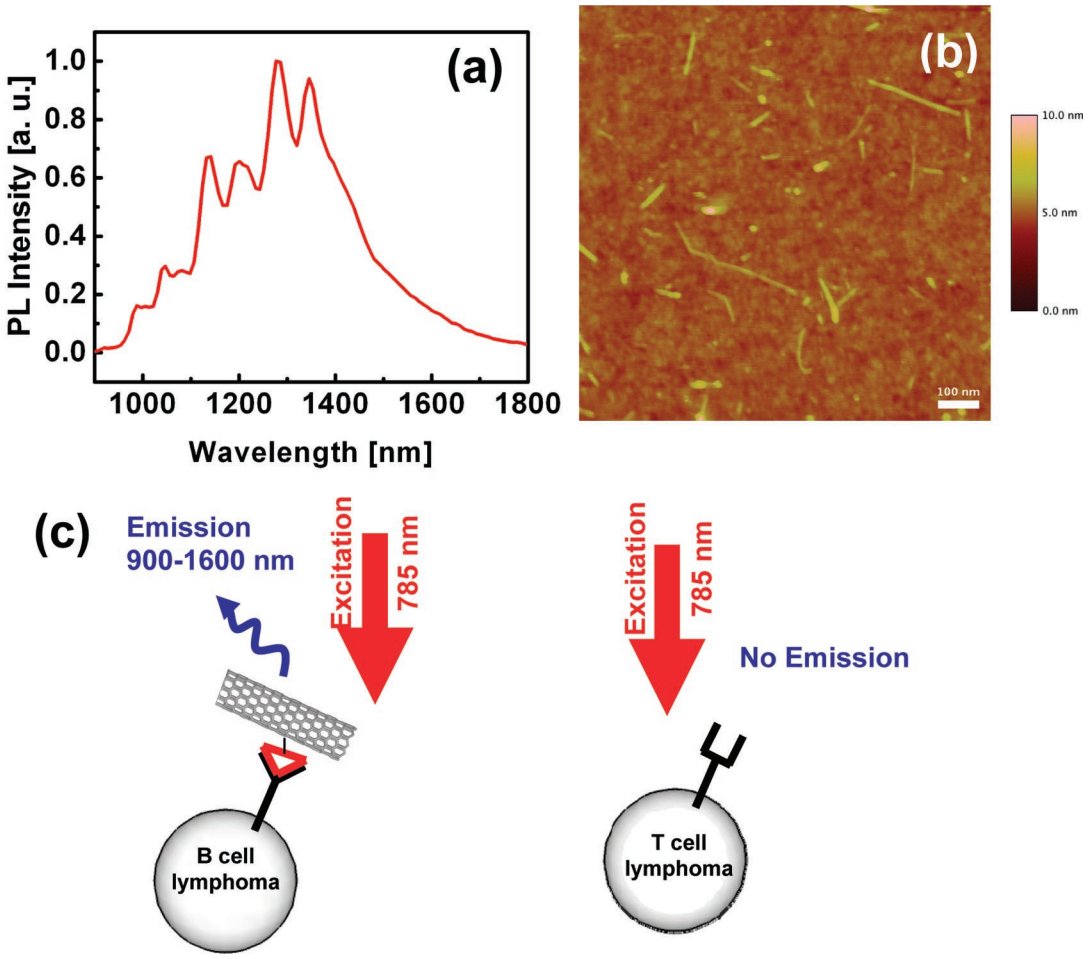

Figure 1. (a) An NIR photoluminescence spectrum of SWNT−Rituxan conjugate, showing typical SWNT emission peaks. (b) AFM image of the PEGylated SWNTs. The average SWNT length was ~83 nm. The average SWNT diameter was found to be 1.6 nm, which is consistent with HiPco SWNTs (average diameter 0.7 − 1.1 nm) that have been well PEGylated. (c) Schematic of NIR photoluminescence (PL) detection of SWNT−Rituxan conjugate selectively bound to CD20 cell surface receptors on B-cell lymphoma (left). The conjugate is not recognized by T-cell lymphoma (right).

antibodies) tagged by nanotubes. To reach this goal, we developed NSB-free, highly water-soluble, short (average length ~50−150 nm, Figure 1b) Hipco SWNTs noncovalently functionalized with PL-PEG-NH_2 with long (~5400D) PEG chains (see Supporting Information). As previously demonstrated,[18] the phospholipid groups strongly adsorb onto the sidewalls of SWNTs and remained intact in biological solutions including serum and in vivo with mice. No detachment from nanotubes was observed owing to strong binding of phospholipids on SWNTs[18] even when under harsh conditions such as heating to high temperatures. The hydrophilic PEG chains extend into the aqueous phase, rendering nanotubes water soluble and free of NSB of biological molecules such as proteins.[15,16,19] Recently, SWNTs functionalized with such long PEG chains were shown to exhibit much reduced NSB to live cells and cellular uptake than SWNTs functionalized with short PEG chains,[17,18] suggesting that the interactions between carbon nanotubes and living cells are strongly dependent on surface functionalization of nanotubes.

To impart biological specificity to the PEGylated nanotubes, we covalently linked the terminal amine groups of PEG chains on SWNTs via sulfosuccinimidyl-4-(*N*-maleimidomethyl)cyclohexane-1-carboxylate (sulfo-SMCC) to thiolated Rituxan antibody specific to CD_{20} cell surface receptor on B-cell lymphomas, or Herception (see Supporting Information), which recognizes the HER2/neu receptor (Figure 1c). The NIR photoluminescence emission spectrum of a solution of SWNT−Rituxan conjugates under 785 nm laser excitation showed peak structures in the 1000−1600 nm region (Figure 1a). These peaks were due to photoluminescence of SWNTs in the Hipco material with certain chiralities (i.e., the (10,3), (10,5), and (9,7) SWNTs) in resonance with the 785 nm laser.[20] This result showed the expected NIR photoluminescence of SWNTs without being affected by antibody conjugation. The measured quantum yield of SWNT photoluminescence is relatively low but can be up to ~3−8%[21−23] by solving extrinsic problems such as bundling. Such quantum yield is sufficient for in vitro NIR imaging applications[12,13] such as the cellular imaging experiments shown here. One of the important advantages of the SWNT fluorophores is the lack of photobleaching[25] without any noticeable decay or loss of photoluminescence intensity even under extended laser excitation.

We incubated B-cells and T-cells in solutions of SWNT−Rituxan conjugates for 1 h at 4 °C to allow the conjugates

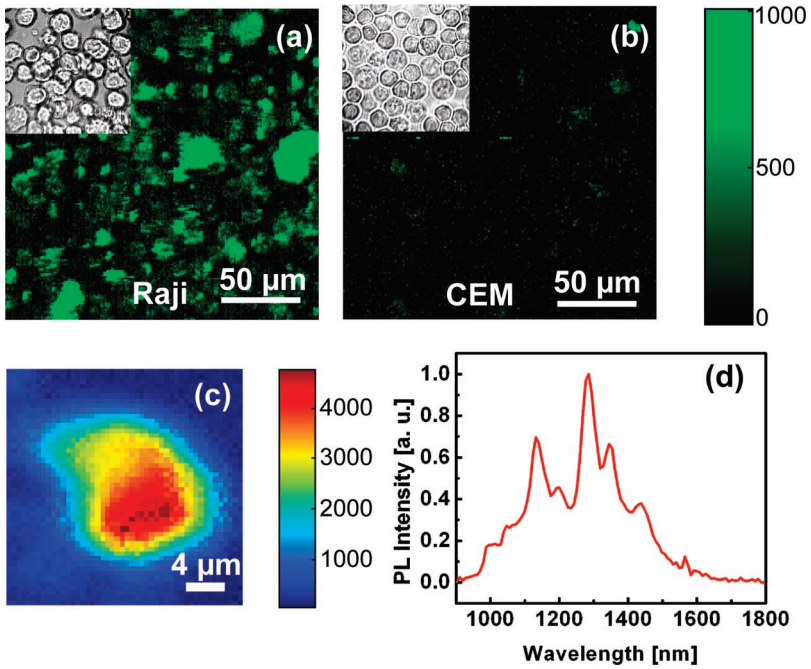

Figure 2. NIR fluorescence images of (a) Raji cells (B-cell lymphoma) and (b) CEM cells (T-cell lymphoma) treated with the SWNT−Rituxan conjugate. Scale bar shows intensity of total NIR emission (in the range of 900−2200 nm). Images are false-colored green. Insets show optical images of cells in the areas. (c) High-magnification NIR fluorescence image of a single Raji cell treated with SWNT−Rituxan conjugate showing NIR fluorescence over the cell. (d) NIR emission spectrum recorded on a SWNT−Rituxan treated Raji cell.

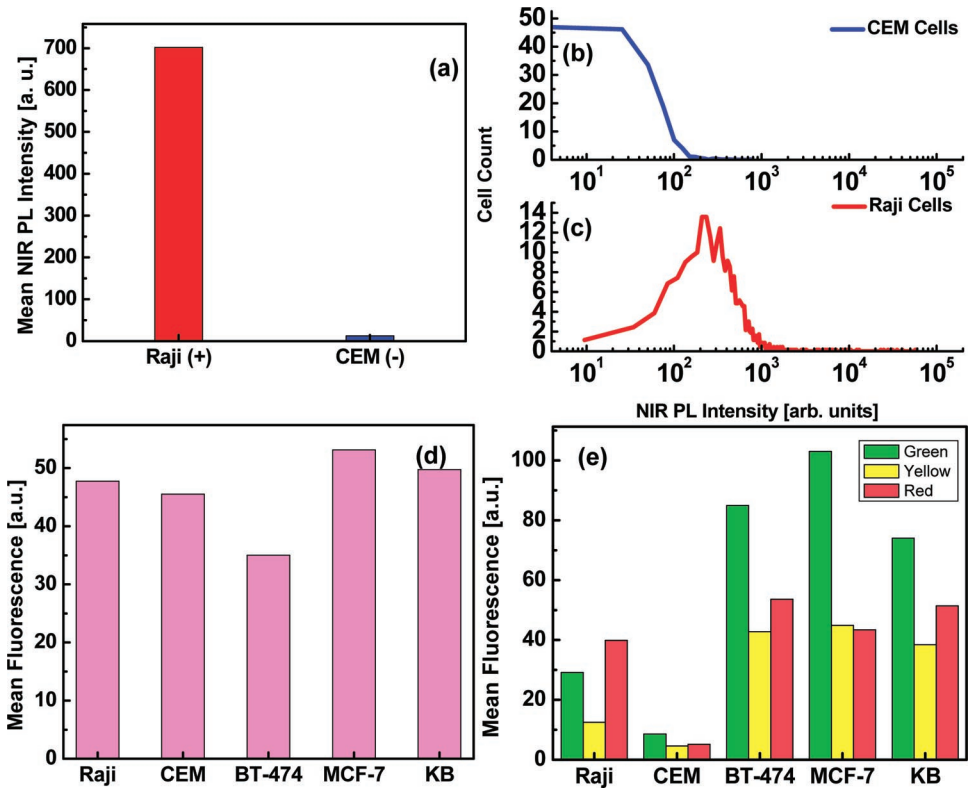

Figure 3. (a) Mean NIR photoluminescence intensity in the image area for both the positive (Raji) and negative (CEM) cells treated by SWNT−Rituxan. (b) Histogram of NIR photoluminescence intensity normalized to number of cell counts for positive and negative cell lines treated by SWNT−Rituxan. Median luminescence counts for Raji and CEM cells are 344 and 10, respectively. (d) Mean autofluorescence in the NIR (total emission in the 900−2200 nm range) of different cell lines (B-cell, T-cell, breast cancer cells, and epidermoid cancer lines, respectively). The values were observed to be low and did not vary significantly between cell lines. This is important when performing high-resolution imaging and for high signal-to-noise imaging. (e) Autofluoresence of various cell lines showing high variability in the visible measured at three emission wavelengths by FACS with a three-color FACScan (Becton Dickinson) at an excitation wavelength of 488 nm. The fluorescence intensities in different fluorescence channels (FL1, FL2, and FL3) were measured. The collected emission wavelengths in FL1−FL3 were 530 nm (green), 585 nm (yellow), and 650 nm (red), respectively.

to interact with the cell surface but block internalization via endocytosis.[26] The cells were then washed and imaged by detecting NIR photoluminescence from 900 to 2200 nm using an InGaAs detector under 785 nm excitation (laser spot size ~4 μm fwhm at a power of ~10mW) with a home-built confocal scanning microscope (see Supporting Information). We observed bright NIR emission of SWNTs on Raji cells (B-cell lymphoma) (Figure 2a), suggesting SWNT−Rituxan binding to CD20 cell surface receptors on Raji cells. An emission spectrum (Figure 2d) taken on a Raji cell (Figure 2c) confirmed that the light collected was coming from SWNTs. In contrast, NIR fluorescence images taken on SWNT−Rituxan-incubated CEM.NKR cells (T-cells, CD20 negative) showed little NIR photoluminescence (Figure 2b), indicating the lack of SWNT−Rituxan binding to T-cells. Control experiments found that our PEGylated SWNTs without Rituxan conjugation exhibited low binding to both B-cells and T-cells (data not shown), confirming the blocking of NSB of SWNTs to cells by PEGylation. These results suggest highly specific binding of our SWNT−Rituxan conjugates to CD20 expressing Raji cells (B-cells), revealed by detecting the intrinsic band gap photoluminescence of SWNTs in the NIR.

To quantify the degree of binding specificity of SWNT−Rituxan to Raji B-cells over CEM T-cells, we allowed the cells to assemble densely until near a monolayer for NIR photoluminescence imaging. Under this condition, the mean pixel value of NIR photoluminescence was directly proportional to the average fluorescence of the cells. We found that the positive/negative ratio between the mean photoluminescence levels of SWNT−Rituxan on Raji and CEM cells was ~55:1 (Figure 3a), demonstrating highly selective recognition of CD20 cell surface receptors by SWNT−Rituxan conjugates and minimal nonspecific binding of the conjugates to the negative cells.

We further analyzed the distribution/histogram of NIR photoluminescence intensity in the images of the cells incubated in solutions of SWNT−Rituxan. By so doing, we gleaned the variations of fluorescence intensity over the cell images (Figure 3b). This was aimed at obtaining information about distribution variations of SWNTs bound to the cells, to mimic data of what one might obtain using visible fluorescent labels in fluorescent-activated cell sorting, or FACS. Note that real FACS should be possible using SWNT NIR tags and FACS instruments equipped with near IR detectors. The Raji sample shows a distribution shifted to higher fluorescence intensity compared to the CEM sample, again indicating higher binding by the positive sample. Large numbers of cells could be investigated this way using SWNTs as NIR tags for cell imaging and probing the specificity of cell surface interactions by measuring large cell populations over large surfaces.

To further establish that our method could be extended to other biological systems, we carried out Herceptin conjugation to SWNTs for recognizing the HER2/neu cell surface receptor overexpressed on various cancer cells and cell imaging by detecting the NIR photoluminescence of nanotubes. The SWNT−Herceptin conjugate was prepared in an

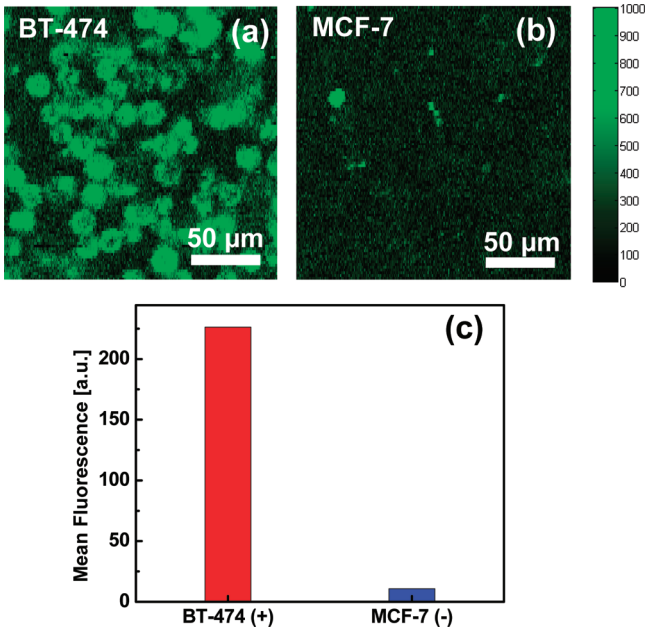

Figure 4. (a) NIR fluorescence image of BT-474 cells, which are HER2/neu positive, treated with the SWNT−Herceptin conjugate. (b) NIR fluorescence image of MCF-7 cells, which are HER2/neu negative, treated with the SWNT−Herceptin conjugate. (c) Mean NIR fluorescence values for the positive and negative cell lines after treatment with the SWNT−Herceptin conjugate, showing a positive/negative ratio of ~20:1.

analogous manner to the SWNT−Rituxan conjugate. The positive cell used was the BT-474 cell line, which is HER2/neu positive. The MCF-7 cell line was used as a negative. The results of NIR fluorescence imaging for the positive and negative cell lines after incubation in SWNT−Herceptin (Figure 4a,b) clearly showed selective binding of nanotube conjugates to the positive cells. Mean photoluminescence values from a high cell density area (Figure 4c) show a positive/negative ratio of ~20:1, suggesting the generality of SWNT−antibody selective binding to specific cell types and the antibodies retaining biological specificity when conjugated to PEGylated SWNTs.

A major advantage of using SWNT as an NIR fluorophore was that SWNT photoluminescence occurs in the 1−2 μm region of little or no cellular autofluorescence. In control experiments, we observed negligible background signals due to autofluorescence of cells in the NIR region compared to SWNT photoluminescence (Figure 3d). Also important was that little variation in the NIR autofluorescence levels was seen between different cell lines. This was advantageous over high autofluorescence levels with large variations between cell lines in the visible region as reported in the literature[1] and observed in our control FACS experiment with several cell lines (Figure 3e). As a result, SWNT NIR tags may allow for highly sensitive detection of low expression levels of cell surface proteins, which could be valuable to various biological and medical applications such as disease diagnosis and assessment of response to therapy at the cellular level.

Highly hydrophilic and inert functionalization of SWNTs to afford no NSB to biological systems is critical to developing SWNT spectroscopic tags. This differs from the

direction of developing SWNTs as molecular transporter for intracellular delivery, for which nanotubes exhibiting high NSB to a wide range of cells are needed to facilitate cellular binding and subsequent internalization/uptake via endocytosis.[17,26] The strategy of high degree of PEGylation followed by ligand or antibody conjugation can also enable selective binding of SWNTs to specific cells for in vitro and in vivo imaging and targeted delivery[11,18] applications.

In summary, we have used the intrinsic band gap NIR fluorescence of SWNTs as a tool to evaluate the recognition of cell surface receptors by antibodies. This established SWNTs as an NIR fluorescent molecule for probing specific binding of biological systems. The functionalization chemistry used here can be easily adapted for a wide range of antibodies or bio-specific ligands, for assaying cell surface proteins in vitro. The SWNT NIR fluorophors exhibit important advantages in low background, which could be used for sensitive molecular detection and imaging at the cellular level and eventually in vivo.

Acknowledgment. This work was supported by NIH−NCI funded CCNE-TR at Stanford (a BioX grant). We are grateful to Drs. Alice Fan, Dean Felsher, and Sanjiv Gamhbir for providing the antibodies used in this work.

Supporting Information Available: PEGylation SWNTs by PL−PEG_{5400}−NH_2, antibody (Rituxan, Herceptin) conjugation on SWNTs, cell culture, and confocal NIR PL imaging of cells. This material is available free of charge via the Internet at http://pubs.acs.org.

References

(1) Aubin, J. E. *J. Histochem. Cytochem.* **1978**, *27*, 36−43.
(2) Friebel, M.; Meinke, M. *J. Biomed. Opt.* **2005**, *10*, 064019.
(3) Michalet, X.; Pinaud, F. F.; Bentolila, L. A.; Tsay, J. M.; Doose, S.; Li, J. J.; Sundaresan, G.; Wu, A. M.; Gambhir, S. S.; Weiss, S. *Science* **2005**, *307*, 538−544.
(4) Wehrenberg, B. L.; Wang, C.; Guyot-Sionnest, P. *J. Phys. Chem. B* **2002**, *106*, 10634−10640.
(5) Kim, S.; Lim, Y. T.; Soltesz, E. G.; DeGrand, A. M.; Lee, J.; Nakayama, A.; Parker, J. A.; Mihaljevic, T.; Laurence, R. G.; Dor, D. M.; Cohn, L. H.; Bawendi, M.; Frangioni, J. V. *Nature Biotech.* **2003**, *22*, 93−97.
(6) O'Connell, M. J.; Bachilo, S. M.; Huffman, C. B.; Moore, V. C.; Strano, M. S.; Haroz, E. H.; Rialon, K. L.; Boul, P. J.; Noon, W. H.; Kittrell, C.; Ma, J. P.; Hauge, R. H.; Weisman, R. B.; Smalley, R. E. *Science* **2002**, *297*, 593−6.
(7) Kam, N. W. S.; Jessop, T. C.; Wender, P. A.; Dai, H. J. *J. Am. Chem. Soc.* **2004**, *126*, 6850−6851.
(8) Dumortier, H.; Lacotte, S.; Pastorin, G.; Marega, R.; Wu, W.; Bonifazi, D.; Briand, J. P.; Prato, M.; Muller, S.; Bianco, A. *Nano Lett.* **2006**, *6*, 1522−1528.
(9) Kam, N. W. S.; O'Connell, M.; Wisdom, J. A.; Dai, H. *Proc. Natl. Acad. Sci. U.S.A.* **2005**, *102*, 11600−11605.
(10) Feazell, R. P.; Nakayama-Ratchford, N.; Dai, H.; Lippard, S. J. *J. Am. Chem. Soc* **2007**, *129*, 8438−8439.
(11) Liu, Z.; Sun, X.; Nakayama-Ratchford, N.; Dai, H. *ACS Nano* **2007**, *1*, 50−56.
(12) Cherukuri, P.; Bachilo, S. M.; Litovsky, S. H.; Weisman, R. B. *J. Am. Chem. Soc.* **2004**, *126*, 15638−15639.
(13) Cherukuri, P.; Gannon, C. J.; Leeuw, T. K.; Schmidt, H. K.; Smalley, R. E.; Curley, S. A.; Weisman, R. B. *Proc. Nat. Acad. Sci. U.S.A.* **2006**, *103*, 18882−18886.
(14) Kam, N. W. S.; Dai, H. *J. Am. Chem. Soc.* **2005**, *127*, 6021−6026.
(15) Shim, M.; Kam, N.; Chen, R.; Li, Y.; Dai, H. *Nano Lett.* **2002**, *2*, 285−288.
(16) Chen, R. J.; Bangsaruntip, S.; Drouvalakis, K. A.; Kam, N. W. S.; Shim, M.; Li, Y. M.; Kim, W.; Utz, P. J.; Dai, H. J. *Proc. Nat. Acad. Sci. U.S.A.* **2003**, *100*, 4984−4989.
(17) Liu, Z.; Winters, M.; Holodniy, M.; Dai, H. J. *Angew. Chem., Int. Ed.* **2007**, *46*, 2023−2027.
(18) Liu, Z.; Cai, W. B.; He, L. N.; Nakayama, N.; Chen, K.; Sun, X. M.; Chen, X. Y.; Dai, H. J. *Nature Nanotechnol.* **2007**, *2*, 47−52.
(19) Chen, R.; Zhang, Y.; Wang, D.; Dai, H. *J. Am. Chem. Soc.* **2001**, 123.
(20) Bachilo, S. M.; Strano, M. S.; Kittrell, C.; Hauge, R. H.; Smalley, R. E.; Weisman, R. B. *Science* **2002**, *298*, 2361−236.
(21) Crochet, J.; Clemens, M.; Hertel, T. *J. Am. Chem. Soc.* **2007**, *129*, 8058−8059.
(22) Carlson, L. J.; Maccagnano, S. E.; Zheng, M.; Silcox, J.; Krauss, T. D. *Nano Lett.* **2007**, *7*, 3698−3703.
(23) Tsyboulski, D. A.; Rocha, J.-D. R.; Bachilo, S. M.; Cognet, L.; Weisman, R. B. *Nano Lett.* **2007**, *7*, 3080−3085.
(24) Perebeinos, V.; Tersoff, J.; Avouris, P. *Phys. Rev. Lett.* **2005**, *94*, 027402.
(25) Arnold, M. S.; Sharping, J. E.; Stupp, S. I.; Kumar, P.; Hersam, M. C. *Nano Lett.* **2003**, *3*, 1549−1554.
(26) Kam, N. W. S.; Liu, Z.; Dai, H. J. *Angew. Chem.* **2005**, *45*, 577−581.

NL072949Q